JOURNAL OF SUSTAINABLE MATERIALS PROCESSING AND MANAGEMENT
e-ISSN: 2821-2843

JSMPM

Vol. 4 No. 2 (2024) 15-23
https://publisher.uthm.edu.my/ojs/index.php/jsmpm

# Preparation and Application of Immobilized Valproic Acid Xerogel as Delivery System

**Ahmed A. Haroun[1]*, Ragab A. Masoud[1], Ali H. M. Osman[2]**

[1] *Chemical Industries Research Division Institute, National Research Centre, 33 El Bohouth Str., Dokki, Giza, EGYPT*
[2] *Department of Organic Chemistry, Faculty of Science, Beni-Suef University, 62514, EGYPT*

*Corresponding Author: haroun68_2000@yahoo.com
DOI: https://doi.org/10.30880/jsmpm.2024.04.02.002

**Article Info**

Received: 12 May 2024
Accepted: 15 July 2024
Available online: 15 August 2024

**Keywords**

Xerogels, hybrid materials, TEOS, valproic acid, in vitro drug release

**Abstract**

The objective of this study is to conduct the preparation and characterization of a xerogel through the co-gelation process involving tetraethyl orthosilicate (TEOS) and 2-propylpentanoic acid (Valproic acid, VA). The characterization of the resulting xerogel utilized techniques such as infrared spectroscopy (FT-IR), X-ray diffraction (XRD), as well as scanning and transmitting electron microscopes (SEM and TEM). Furthermore, the in vitro release of VA and the kinetics of its release were investigated employing various mathematical models (zero-order, first-order, and Higuchi) in a phosphate buffer solution at pH 7.4 and 37°C utilizing HPLC. The findings from the FTIR and XRD analyses provided evidence supporting the successful synthesis of the xerogel with an amorphous configuration. Nevertheless, observations from TEM images exhibited a spherical-like morphology with an average dimension of approximately 1910 d.nm, contrasting with the pure TEOS measuring 924 d.nm. Moreover, the research illustrated a regulated release of VA after 4 h, indicating that the TEOS-based xerogel presents a promising approach for VA delivery characterized by sustained release following the Higuchi kinetic over a 24-h period. Subsequent to these outcomes, the xerogel with an amorphous configuration was successful synthesized for VA regulated release.

## 1. Introduction

Xerogels are produced via a sol-gel technique that commonly includes low-temperature synthesis, which renders it a method that is both energy-efficient and eco-friendly, thereby contributing to sustainability in material processing. The incorporation of xerogels in drug delivery systems enables the precise and prolonged release of active pharmaceutical ingredients, thus diminishing the necessity for frequent administration and decreasing the potential environmental repercussions stemming from excessive drug discharge. They can be customized to encapsulate diverse substances, promoting the efficient utilization of materials and diminishing wastage in various applications like drug delivery and catalysis, thereby aligning with the fundamental principles of sustainability in material design and usage. Moreover, the organic-inorganic hybrid materials are currently attracting significant attention from researchers because of the synergistic interactions between the two constituents, resulting in distinct properties suitable for a wide range of applications [1-4]. Among these hybrid materials, organically modified silicates are particularly notable for their diverse morphologies, porous structures, and surface chemical characteristics, making them versatile options for coatings on various substrates [5-7]. The sol-gel technique, a well-established method, is utilized in the production of silicon hybrid xerogels; this method is distinguished by its straightforwardness, mild operational conditions, and the capacity

to customize materials with a variety of properties through adjustments in synthesis parameters such as water content, monomer ratios, gelling and drying temperatures, catalyst concentration, and pH levels within the synthesis environment. Previous studies have illustrated the utilization of tetraethyl orthosilicate (TEOS) as a precursor for $SiO_2$ in numerous sol-gel hybrid composite formulations [9]. Recent progress in nanotechnology has transformed the delivery of drugs to specific organs for various medical conditions. The use of drug-loaded nanoparticles presents numerous advantages over traditional dosage forms, including enhanced solubility, protection of cargo, sustained drug release, and targeted delivery, ultimately amplifying the therapeutic effectiveness of medications [10-14]. The examination of nanoparticle behavior in vitro is often centered around on the contentious aspect of the release study. Understanding the in vitro release kinetics of nanoparticles is crucial as it provides valuable insights into their ability to impact drug release, thus becoming a key consideration in the assessment of material safety, efficacy, and quality. When conducted appropriately, these studies can be linked to in vivo behavior using predictive mathematical models [15,16], leading to accelerated regulatory approval. Valproic acid (VA) and sodium valproate (VAS) are commonly utilized anticonvulsants for the management of various types of absence seizures, both simple and complex. VA, known for its chemical stability under different conditions like heat, light, strong aqueous alkali, or acid exposure, is highly valued for its reliability [17]. With broad-spectrum efficacy against different types of epileptic conditions, VA plays a significant role as an antiepileptic medication [18]. Recent research efforts have highlighted the notable anti-tumor properties of VA in different in vitro and in vivo scenarios, suggesting its potential as a cancer treatment option [19,20]. Despite its wide range of antiepileptic advantages, the use of VA is limited due to occasional but severe adverse reactions [21-24]. Compared to other antiepileptic medications, VA has the shortest half-life, typically lasting between 10 to 15 h [25]. Strategies involving pharmacological and chemical interventions are implemented to manage fluctuations in the medication's plasma levels [26,27]. However, a method for producing a xerogel matrix embedding VA coating with TEOS using the sol-gel technique has not been clearly defined. This study seeks to create and analyze a hybrid xerogel containing TEOS and VA. The development of a surfactant-free hybrid xerogel has not been explored yet. Various analytical methods such as Infrared spectroscopy (FT-IR), X-ray diffraction (XRD), scanning electron microscopy (SEM), and transmission electron microscopy (TEM) were employed to elucidate the properties of the xerogel. Furthermore, the cumulative release of VA in vitro and its release kinetics in a phosphate buffer at pH 7.4 and 37°C were assessed through HPLC analysis.

## 2. Materials and Methods

### 2.1 Materials

Convulex® valproic acid (VPA) were obtained from Aldrich (USA). Tetraethyl orthosilicate (TEOS, 99%) purchased from Sigma-Aldrich. The chemicals and reagents such as: phosphate buffer, potassium dihydrogen phosphate (98%, $KH_2PO_4$), triethylamine (99.7%), and ortho-phosphoric acid (33%) were obtained by Thermo Fisher Scientific. The other ones were used as received from local resources.

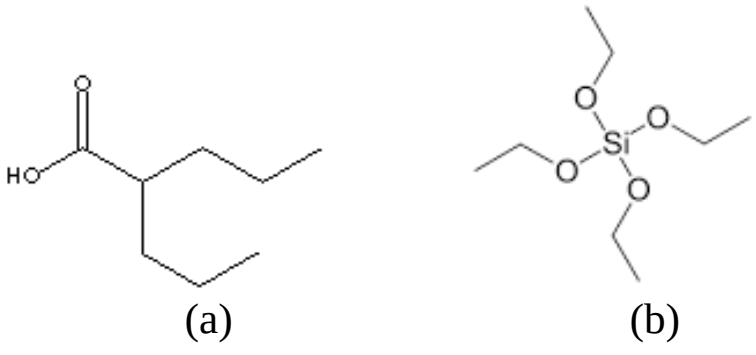


**Fig. 1** *Chemical structures of (a) VA; (b) TEOS*

### 2.2 Methods

#### 2.2.1 Preparation of VA-Immobilized Xerogel

The alkoxides precursor utilized was tetraethyl orthosilicate, which was acquired from ABCR (TEOS, 99%), along with sodium nitrate acting as a surfactant, obtained from Aldrich. All other precursors employed were of analytical grade and procured from Aldrich. The preparation of silica sol entailed the mixture of TEOS, EtOH, $H_2O$, and hydrochloric acid (HCl). Subsequently, $NaNO_3$ was introduced to the initial solution and agitated for a

duration of 15 min. Following this, ethylene diamine was slowly added drop by drop with continuous stirring for 2 h at room temperature. The solution immediately turned opaque, signaling the commencement of the reaction. The resultant white powder precipitate was then filtered and rinsed with deionized water, after which the particles were air-dried overnight at room temperature.

### 2.2.2 Characterization

The materials' FT-IR spectra were obtained using KBr pellets on a Vertex 70 Model (Germany) FT-IR spectroscopy system with the following parameters: scan resolution: 4 $cm^{-1}$, scan rate: 2 mm/s, scan count: 32, range: 400-4000 $cm^{-1}$, and mode: Transmission. The Rigaku Miniflex was used to create X-ray diffraction patterns (XRD) with Cu (Kα 30 kV, 15 mA, λ = 1.54178 Å) radiation. The samples' TEM images were taken using a JEOL transmission electron microscope JEM-1230. The SEM micrographs were examined using a JEOL analytical scanning electron microscope, JSM-6510LA.

### 2.2.3 In Vitro VA Released Study

To determine the rate of VA release from xerogel, 200 mg of the formulation was put in a glass test tube containing 10 mL of phosphate buffer pH 7.4 (PB) and 0.1% twin 80 to provide sink conditions, with 200 rpm agitation. A 1 mL sample was taken at predetermined intervals of 0.05, 0.25, 1, 4, and 24 h and replaced with fresh PB at 37°C. The VA content of the samples was determined using the HPLC technique described [28-30]. An Agilent 1200 Series High Performance Liquid Chromatography (HPLC) system was used for chromatographic conditions and quantification, which included a degasser (G1322A), a gradient pump (G1311A), an autosampler (G1329A), and a dido array detector (G1315B). Separation was performed using a reversed-phase C18 analytical column packed at 5 m ps. ODS (250 mm x 4.6 mm id). At measure VPA, the dido array detector was set at 213 and 230 nm. Furthermore, the mobile phase included 20 mM potassium dihydrogen phosphate ($KH_2PO_4$) and 0.1% triethylamine, and the pH was adjusted to 4.0 using ortho-phosphoric acid (1M), at a flow rate of 1.2 mL per min.

## 3. Results and Discussion

### 3.1 Physicochemical Characterization

The interaction between VA and TEOS was validated using FTIR-ATR spectroscopy. Fig. 2 shows the spectrum data. The VA/TEOS sample, like pure TEOS, had the anticipated functional groups. In other words, the different peaks at 3100, 2940, and (1310-1460) $cm^{-1}$ correspond to the aliphatic stretching of -$CH_2$, -CH, and in-plane bending vibrations of C-H bonds (alkyl groups), respectively. Furthermore, the distinctive peaks at 1640 and 1735 $cm^{-1}$ represent the carbonyl ester groups' -$CH_2$ bending vibrations and -C=O stretching, respectively. These peaks are definitely caused by VA-TEOS interactions during sol-gel synthesis. The carboxylic acid groups at VA have been effectively attached to the TEOS, as demonstrated by the broad band at 3460 $cm^{-1}$, which corresponds to the stretching vibration bonds of O-H groups. Following sol-gel manufacturing, additional differentiating wear peaks appeared around (1150-1210) and (600-800) $cm^{-1}$, corresponding to the functional groups Si-O-Si and Si-C (Si-$CH_2$). Minor peaks at 490 and 960 $cm^{-1}$, corresponding to the O-Si-O and Si-OH groups, appeared as predicted throughout the TEOS hydrolysis process [31,32]. The results, which are consistent with our previous work, reveal that various amino acids may connect covalently with ox-MWCNTs using the sol-gel approach [33,34].

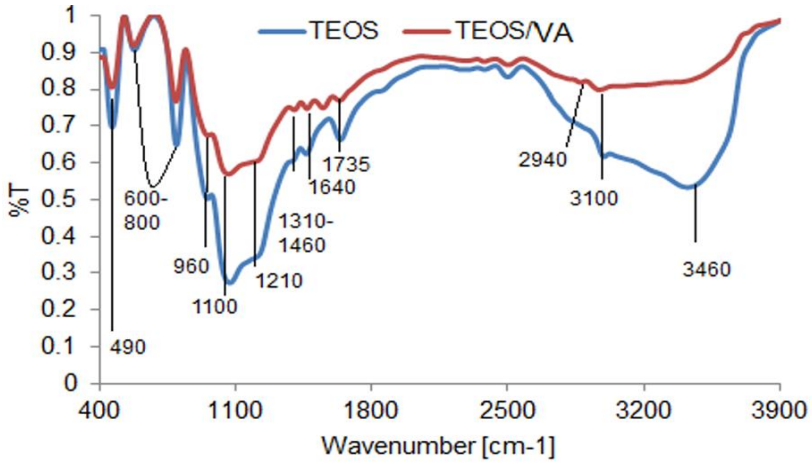


**Fig. 2** *FTIR spectra of VA/TEOS xerogel in compared with pure TEOS*

Fig. 3 shows TEM pictures of (a) VA/TEOS xerogel, (b) pure TEOS, and a SEM micrograph of VA/TEOS xerogel. When TEOS was used as a silica precursor in the sol-gel process, the particles formed were spherical, as predicted [42]. Following VA integration, particle aggregation with spherical shape may occur. In the absence of VA, the hydrolysis and subsequent condensation of TEOS produce spherical silica particles. Bele et al. [36] previously cited an example of such material produced at the conditions used in the current study. However, in the presence of VA particles, silica forms a thin coating on their surfaces (Fig. 3c).

According to Park et al. [37], a high-water concentration causes a high nucleation rate, resulting in a huge number of subparticles in a short period of time. However, because to the extra water, the hydrogen bond between $SiO_2$ subparticles is stronger at higher water concentrations than at lower ones. As a result of the agglomeration, larger particles (average size 1910 d.nm) form in compared to pure TEOS (924 d.nm).

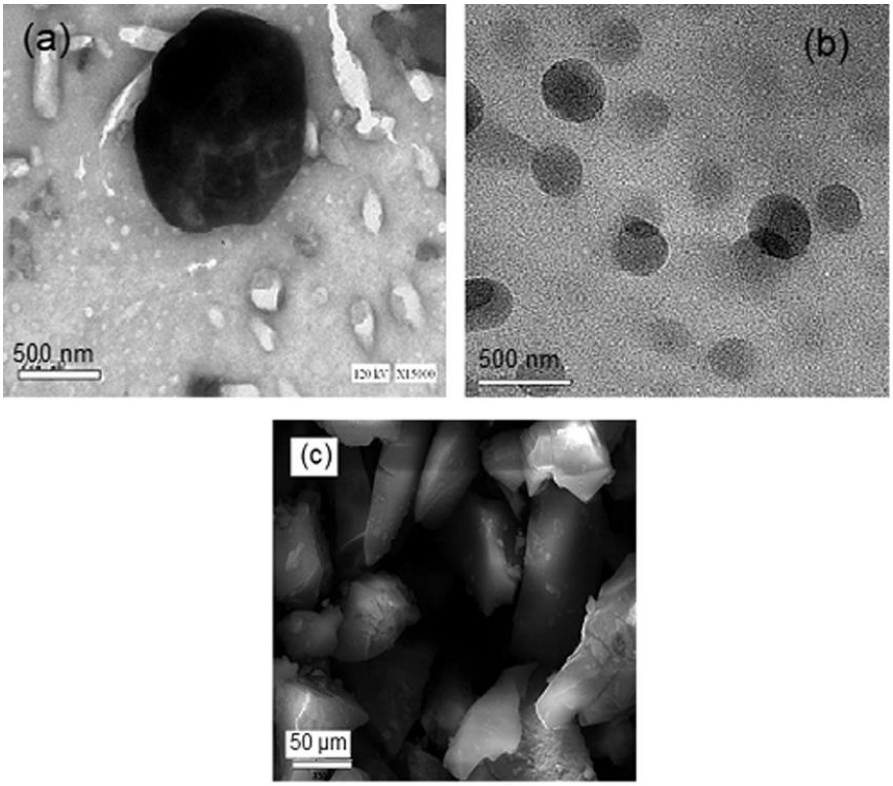


**Fig. 3** *TEM images of (a) VA/TEOS xerogel; (b) pure TEOS; and (c) SEM-micrograph of VA/TEOS xerogel (at scale bar 500 nm+15 Kv and 50 µm+ for TEM and SEM, respectively)*

As seen in Fig. 4, XRD was used to monitor the phase formation process in a silica matrix (VA-TEOS xerogel) generated by the sol-gel technique. The as-dried gel, which corresponds to the amorphous silica matrix, has a substantially wider peak in the 2θ range of 20-28° [38]. This means that no crystalline phase developed during the first room-temperature drying of VA-prepared xerogel.

J. of Sustainable Materials Processing and Management Vol. 4 No. 2 (2024) p. 15-23

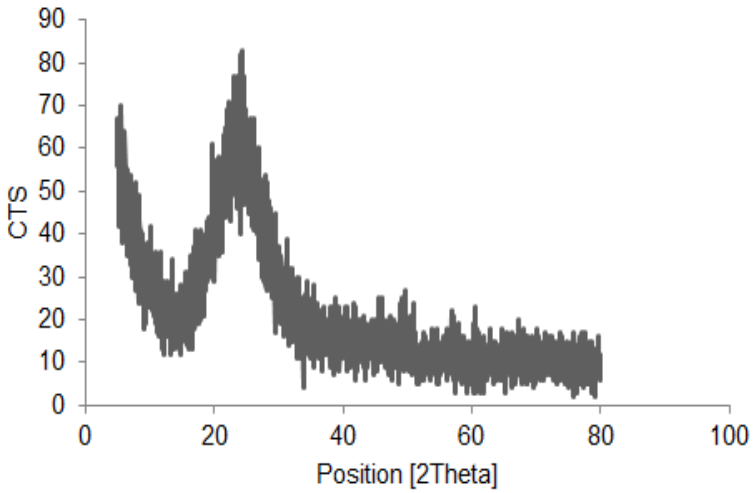


**Fig. 4** *XRD patterns of VA/TEOS xerogel*

## 3.2 In Vitro VA Release Profile and Kinetics of Release Assessment

Numerous investigations in the past have delved into diverse techniques for the immobilization of Valproic acid (VA) on distinct carriers. One particular study was centered on the formulation of a robust solid dosage form for VA utilizing carriers such as AEROSIL® 300 Pharma and AEROPERL® 300 Pharma, leading to elevated drug loading and exceptional dissolution characteristics [39]. Moreover, exploration has assessed innovative solid VA formulations crafted via cyclodextrins complexation and solid dispersion techniques, demonstrating enhanced solubility and dissolution profiles akin to VA sodium salt, albeit with variances in pharmacological assessments [40]. Additionally, an approach employing molecularly imprinted polymer fiber in combination with chromatography-flame ionization effectively identified VA in diverse samples, presenting notable sensitivity and selectivity [41]. These collective studies afford valuable insights into diverse strategies and constraints in immobilizing VA on different carriers to enhance stability, detection, and solubility.

An HPLC system was used to conduct in vitro dissolution tests. The percentage release of VA from TEOS conjugate on hydrolysis was estimated by comparing the drug's peak area to the standard VA calibration graph. It hydrolyzed slowly at pH 7.4. The findings revealed that in vitro VA release was acid-free and stable in acidic conditions. These findings are similar with previous studies by Praveen et al [42], who investigated in vitro VA release from a VA-dextran combination at various buffer pH values.

The in vitro VA release profile from the VA/TEOS xerogel was collected and analyzed using phosphate buffer at 37°C for 24 h, as shown in Fig. 5. During the first 4 hours, there was a burst of VA release from the formulation, which might be attributable to the presence of carbonyl ester groups on VA side chains, which improved swellability and consequently increased VA diffusion. As previously noted, increasing the carboxylic content of the structure improved drug adsorption [43,44]. This has been clarified by adding additional particular acidic groups to the network that have a high swelling ability. In other words, the carboxylic groups on the side chains became ionized, allowing the structure to extend upward. It was demonstrated that steady-state serum concentrations of valproic acid in two sustained-release formulations were different because of the different dissolution profiles, and prescribers should be aware that the therapeutic drug monitoring data are not consistent [45].

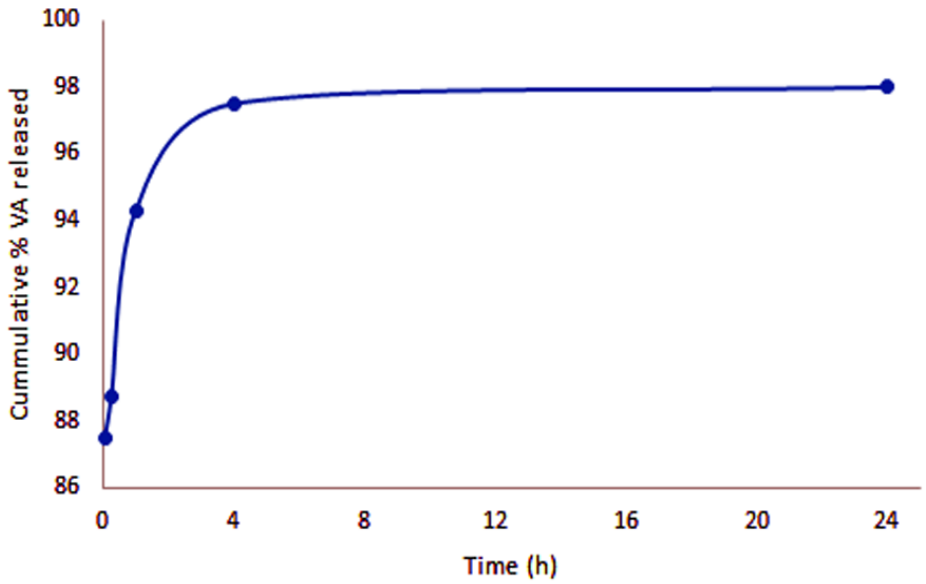


**Fig. 5** *In vitro cumulative VA release profile at different interval of time in phosphate buffer pH 7.4, from the VA/TEOS xerogel at 37°C*

Furthermore, TEOS' hydrophilicity and short contact angle increased solubility in aqueous environments. As a result, VA dispersion has risen [46]. After 4 h, the VA profile remained steady. This behavior might be explained by the existence of an equilibrium in the network aqueous phase between free VA and VA/TEOS complexed molecules. To evaluate the kinetic VA released, three mathematical models (zero-order, first-order, and Higuchi) were applied. Linear regression analysis was performed to determine each model's kinetic rate constants (k). Furthermore, the correlation coefficient ($R^2$) was measured to determine the fitness's accuracy.

Table 1 displays the kinetic rate constants (k) and correlation coefficients ($R^2$). In compared to the other zero-order and first-order models ($R^2$ = 0.434 and 0.562, respectively), the Higuchi model showed the greatest fit ($R_2$ = 0.639) for describing the VA release from the xerogel.

**Table 1** *Kinetic parameters of the in vitro VA release from xerogel*

| Kinetic model | Rate constant (K) | $R^2$ |
|---|---|---|
| Zero-order | 0.313 | 0.434 |
| First-order | 0.027 | 0.562 |
| Higuchi | 2.06 | 0.639 |

## 4. Conclusions

The application of the sol-gel method proved to be effective in the encapsulation of Valproic acid (VA) within Tetraethyl Orthosilicate (TEOS). Diverse analytical methodologies such as FTIR, XRD, TEM, and SEM were utilized to confirm the formation of the resulting xerogel. Under the conditions of phosphate buffer pH 7.4 at 37 °C, the release of VA displayed sustained behavior in accordance with the Higushi kinetic model over a period of 24 h. The results obtained from the FTIR and XRD examinations provided evidence supporting the successful fabrication of the xerogel in an amorphous state. Analysis of TEM images exhibited a spherical morphology of the xerogel with an average size of around 1910 nanometers, contrasting with the pure TEOS particles measuring 924 nanometers. The controlled release of VA observed after 4 h suggests that the TEOS-based xerogel offers a promising strategy for the delivery of VA. Subsequent investigations are warranted to compare the efficacy of various administration routes for delivering valproic acid.

## Acknowledgement

The authors are thankful to National Research Centre, Giza, Egypt for supporting this work.

## Conflict of Interest

Authors declare that there is no conflict of interests regarding the publication of the paper.

## Author Contribution

*The authors confirm contribution to the paper as follows:* ***study conception and design:*** *Ahmed A. Haroun, Ragab A. Masoud, Ali Osman;* ***data collection:*** *Ahmed A. Haroun, Ragab A. Masoud, Ali Osman;* ***analysis and interpretation of results:*** *Ahmed A. Haroun, Ragab A. Masoud, Ali Osman;* ***draft manuscript preparation:*** *Ahmed A. Haroun, Ragab A. Masoud. All authors reviewed the results and approved the final version of the manuscript.*

## References

[1] Kumar, S. A., Shankar, J. S., Gouthaman, S., & Periyasamy, B. K. (2023). Effect of electrosteric stabilization of TiO2 nanoparticles on photophysical properties of organic/inorganic hybrid nanocomposite. Materials Today Communications, 35, 105533. https://doi.org/10.1016/j.mtcomm.2023.105533

[2] Lin, C. B., Sun, F. L., Wen, J., Chen, W. X., & Zhuang, G. L. (2023). Rational design of one inorganic-organic hybrid Z-scheme heterojunction for high-performance photocatalytic water splitting. Fuel, 341, 127682. https://doi.org/10.2139/ssrn.4313244

[3] Su, G., Liang, Z., Zhong, J., Ning, H., Lu, K., Qiu, T., ... & Peng, J. (2023). Solution-processed, flexible, and highly transparent ZrO2: PVP hybrid dielectric layer. Organic Electronics, 116, 106759. https://doi.org/10.1021/ja107079d

[4] Zhou, Y. Q., Zhou, Y., Li, J. T., Zanna, S., Seyeux, A., Marcus, P., & Światowska, J. (2023). Probing Mg anode interfacial and corrosion properties using an organic/inorganic hybrid electrolyte. Applied Surface Science, 614, 156070. https://doi.org/10.1016/j.apsusc.2022.156070

[5] Uc-Fernández, E., González-Sánchez, J., Ávila-Ortega, A., Pérez-Padilla, Y., Cervantes-Uc, J. M., Reyes-Trujeque, J., & Talavera-Pech, W. A. (2023). Anticorrosive properties of a superhydrophobic coating based on an ORMOSIL enhanced with MCM-41-HDTMS nanoparticles for metals protection. Journal of Coatings Technology and Research, 20(1), 347-357. https://doi.org/10.1007/s11998-022-00675-1

[6] Scotland, K. M., Shetranjiwalla, S., & Vreugdenhil, A. J. (2020). Curable hybrid materials for corrosion protection of steel: Development and application of UV-cured 3-methacryloxypropyltrimethoxysilane-derived coating. Journal of Coatings Technology and Research, 17, 977-989. https://doi.org/10.1007/s11998-019-00317-z

[7] Zarzuela, R., Carbú, M., Gil, A., Cantoral, J., & Mosquera, M. J. (2021). Incorporation of functionalized Ag-TiO2NPs to ormosil-based coatings as multifunctional biocide, superhydrophobic and photocatalytic surface treatments for porous ceramic materials. Surfaces and Interfaces, 25, 101257. https://doi.org/10.1016/j.surfin.2021.101257

[8] Pietras-Ożga, D., Piątkowska-Sawczuk, K., Duro, G., Pawlak, B., Stolyarchuk, N., Tomina, V., ... & Barczak, M. (2022). Sol-gel–derived silica xerogels: Synthesis, properties, and their applicability for removal of hazardous pollutants. Advanced Materials for Sustainable Environmental Remediation, 261-277. https://doi.org/10.3390/gels9050382

[9] Haroun, A. A., Ayoob, F. A., & Masoud, R. A. (2024). Sol-Gel Immobilization of Colistin Sulfate onto Double Walled Carbon Nanotubes: In Vitro Bone Bioactivity. Nano Biomedicine and Engineering. http://doi.org/10.26599/NBE.2024.9290088

[10] Haroun, A. A., Elnahrawy, A. M., & Abd-Alla, H. I. (2017). Sol-gel preparation and in vitro cytotoxic activity of nanohybrid structures based on multi-walled carbon nanotubes and silicate. Inorganic and Nano-Metal Chemistry, 47(7), 1023-1027. https://doi.org/10.1080/24701556.2017.1284087

[11] Weng, J., Tong, H. H., & Chow, S. F. (2020). In vitro release study of the polymeric drug nanoparticles: development and validation of a novel method. Pharmaceutics, 12(8), 732. https://doi.org/10.3390/pharmaceutics12080732

[12] Haroun, A., Osman, A., Ahmed, S., & Elghandour, A. H. (2022). Synthesis and characterization of ibuprofen delivery system based on β-cyclodextrin/Itaconic acid copolymer. Trends in Sciences, 19(19), 5825-5825. https://doi.org/10.48048/tis.2022.5825

[13] Haroun, A., Osman, A., Ahmed, S., & Elghandour, A. (2019). Beta-cyclodextrin grafted with poly (ε-caprolactone) for ibuprofen delivery system. Egyptian Journal of Chemistry, 62(5), 827-835. https://doi.org/10.21608/EJCHEM.2018.5125.1455

[14] Haroun, A. A., El-Halawany, N. R., Loira-Pastoriza, C., & Maincent, P. (2014). Synthesis and in vitro release study of ibuprofen-loaded gelatin graft copolymer nanoparticles. Drug development and industrial pharmacy, 40(1), 61-65. https://doi.org/10.3109/03639045.2012.746359

[15] Haroun, A. A., & El-Halawany, N. R. (2010). Encapsulation of bovine serum albumin within β-cyclodextrin/gelatin-based polymeric hydrogel for controlled protein drug release. Irbm, 31(4), 234-241. https://doi.org/10.1016/j.irbm.2010.02.001

[16] Cardot, J., Beyssac, E., & Alric, M. (2007). In vitro-in vivo correlation: importance of dissolution in IVIVC. Dissolution technologies, 14(1), 15. https://doi.org/10.14227/DT140107P15

[17] Sjögren, E., Abrahamsson, B., Augustijns, P., Becker, D., Bolger, M. B., Brewster, M., ... & Langguth, P. (2014). In vivo methods for drug absorption–comparative physiologies, model selection, correlations with in vitro methods (IVIVC), and applications for formulation/API/excipient characterization including food effects. European Journal of Pharmaceutical Sciences, 57, 99-151. https://doi.org/10.1016/j.ejps.2014.02.010
[18] Chang, Z. L. (1979). Sodium valproate and valproic acid. In Analytical profiles of drug substances (Vol. 8, pp. 529-556). Academic Press. https://doi.org/10.4103/0250-474X.65026
[19] Zaccara, G., Messori, A., & Moroni, F. (1988). Clinical pharmacokinetics of valproic acid—1988. Clinical pharmacokinetics, 15, 367-389. https://doi.org/10.2165/00003088-198815060-00002
[20] Levy, R. H., & Shen, D. D. In: Levy, R.H., Dreifuss, F.E., Mattson, R.H., Meldrum, B.S., & Penry, J.K. (Eds.), In antiepileptic Drugs. Reven Press, New York, (1989) pp. 583-600.
[21] Duenas-Gonzalez, A., Candelaria, M., Perez-Plascencia, C., Perez-Cardenas, E., de la Cruz-Hernandez, E., & Herrera, L. A. (2008). Valproic acid as epigenetic cancer drug: preclinical, clinical and transcriptional effects on solid tumors. Cancer treatment reviews, 34(3), 206-222. https://doi.org/10.1016/j.ctrv.2007.11.003
[22] Sobol, E., Bialer, M., & Yagen, B. (2004). Tetramethylcyclopropyl analogue of a leading antiepileptic drug, valproic acid. Synthesis and evaluation of anticonvulsant activity of its amide derivatives. Journal of medicinal chemistry, 47(17), 4316-4326. https://doi.org/10.1021/jm0498351
[23] Grauso-Eby, N. L., Goldfarb, O., Feldman-Winter, L. B., & McAbee, G. N. (2003). Acute pancreatitis in children from valproic acid: case series and review. Pediatric neurology, 28(2), 145-148. https://doi.org/10.1016/s0887-8994(02)00517-9
[24] Bryant III, A. E., & Dreifuss, F. E. (1996). Valproic acid hepatic fatalities. III. US experience since 1986. Neurology, 46(2), 465-469.
[25] Bohan, T. P., Helton, E., McDonald, I., Konig, S., Gazitt, S., Sugimoto, T., ... & Koch, G. (2001). Effect of L-carnitine treatment for valproate-induced hepatotoxicity. Neurology, 56(10), 1405-1409. https://doi.org/10.1212/wnl.56.10.1405
[26] Badir, K., Haj-Yehia, A., Vree, T. B., van der Kleijn, E., & Bialer, M. (1991). Pharmacokinetics and anticonvulsant activity of three monoesteric prodrugs of valproic acid. Pharmaceutical research, 8, 750-753. https://doi.org/10.1023/a:1015854118110
[27] Bialer, M., Friedman, M., Dubrovsky, J., Raz, I., & Abramsky, O. (1985). Pharmacokinetic evaluation of novel sustained-release dosage forms of valproic acid in humans. Biopharmaceutics & drug disposition, 6(4), 401-411. https://doi.org/10.1002/bdd.2510060406
[28] Dural, E., Çelebi, S., Bolayır, A., & Çiğdem, B. (2020). Development and validation of a new HPLC method for valproic acid determination in human plasma and its application to a therapeutic drug monitoring study. Macedonian Pharmaceutical Bulletin, 66(10.33320). https://doi.org/10.33320/maced.pharm.bull.2020.66.01.001
[29] Gao, S., Miao, H., Tao, X., Jiang, B., Xiao, Y., Cai, F., ... & Chen, W. (2011). LC–MS/MS method for simultaneous determination of valproic acid and major metabolites in human plasma. Journal of Chromatography B, 879(21), 1939-1944. https://doi.org/10.1016/j.jchromb.2011.05.022
[30] Amini, H., Javan, M., & Ahmadiani, A. (2006). Development and validation of a sensitive assay of valproic acid in human plasma by high-performance liquid chromatography without prior derivatization. Journal of Chromatography B, 830(2), 368-371. https://doi.org/10.1016/j.jchromb.2005.11.028
[31] Avilés, F., Cauich-Rodríguez, J. V., Rodríguez-González, J. A., & May-Pat, A. (2011). Oxidation and silanization of MWCNTs for MWCNT/vinyl ester composites. Express polymer letters, 5(9). https://doi.org/10.3144expresspolymlett2011.75
[32] Goyanes, S., Rubiolo, G. R., Salazar, A., Jimeno, A., Corcuera, M. A., & Mondragon, I. (2007). Carboxylation treatment of multiwalled carbon nanotubes monitored by infrared and ultraviolet spectroscopies and scanning probe microscopy. Diamond and related materials, 16(2), 412-417. 10.1016/j.diamond.2006.08.021
[33] Haroun, A., Gospodinova, Z., & Krasteva, N. (2021). Amino acid functionalization of multi-walled carbon nanotubes for enhanced apatite formation and biocompatibility. Nano Biomed. Eng, 13(4), 380-393. https://doi.org/10.5101/nbe.v13i4.p380-393
[34] Haroun, A. A., Ayoob, F. A., & Masoud, R. A. (2023). Organic-Inorganic Composites Based on Multi-walled Carbon Nanotubes Containing Lysine/Histidine. Egyptian Journal of Chemistry, 66(6), 499-510. https://doi.org/10.21608/ejchem.2023.212461.8004
[35] Rao, K. S., El-Hami, K., Kodaki, T., Matsushige, K., & Makino, K. (2005). A novel method for synthesis of silica nanoparticles. Journal of colloid and interface science, 289(1), 125-131. https://doi.org/10.1016/j.jcis.2005.02.019

[36] Bele, M., Dmitrašinovič, Đ., Planinšek, O., Salobir, M., Srčič, S., Gaberšček, M., & Jamnik, J. (2005). Silica coatings on clarithromycin. International journal of pharmaceutics, 291(1-2), 149-153. https://doi.org/10.1016/j.ijpharm.2004.07.052

[37] Park, S. K., Do Kim, K., & Kim, H. T. (2002). Preparation of silica nanoparticles: determination of the optimal synthesis conditions for small and uniform particles. Colloids and Surfaces A: Physicochemical and Engineering Aspects, 197(1-3), 7-17. https://doi.org/10.1016/S0927-7757(01)00683-5

[38] Zhou, Z. H., Xue, J. M., Wang, J., Chan, H. S. O., Yu, T., & Shen, Z. X. (2002). NiFe 2 O 4 nanoparticles formed in situ in silica matrix by mechanical activation. Journal of applied physics, 91(9), 6015-6020. https://doi.org/10.1063/1.1462853

[39] Khetarpal, N. A., Ramachal, A. K. S., Rao, L., & Amin, P. D. (2012). Formulation development of a stable solid oral dosage form of Valproic acid using colloidal silica. International Journal of Drug Delivery, 4(2), 266.

[40] Trapani, G., Cutrignelli, A., Latrofa, A., Franco, M., Serra, M. A. R. I. A. N. G. E. L. A., Pisu, M. G., ... & Liso, G. (2004). Valproic Acid‐Hydrophilic Cyclodextrin Complexes and Valproic Acid‐Solid Dispersions: Evaluation of Their Potential Pharmaceutical Use. Drug development and industrial pharmacy, 30(1), 53-64. https://doi.org/10.1081/DDC-120027511

[41] Zakerian, R., & Bahar, S. (2019). Molecularly imprinted based solid phase microextraction method for monitoring valproic acid in human serum and pharmaceutical formulations. Journal of the Iranian Chemical Society, 16, 741-745. https://doi.org/10.1007/S13738-018-1551-4

[42] Praveen, B., Shrivastava, P., & Shrivastava, S. K. (2009). In-Vitro release and pharmacological study of synthesized valproic acid-dextran conjugate. ACTA Pharmaceutica Sciencia, 51(2).

[43] gounder Subramanian, K., & Vijayakumar, V. (2012). Synthesis and evaluation of chitosan-graft-poly (2-hydroxyethyl methacrylate-co-itaconic acid) as a drug carrier for controlled release of tramadol hydrochloride. Saudi Pharmaceutical Journal, 20(3), 263-271. https://doi.org/10.1016/j.jsps.2011.09.004

[44] Nayak, A., & Jain, A. (2011). In vitro and in vivo study of poly (ethylene glycol) conjugated ibuprofen to extend the duration of action. Scientia Pharmaceutica, 79(2), 359-374. https://doi.org/10.3797/scipharm.0911-07

[45] Yasui-Furukori, N., Saito, M., Nakagami, T., Niioka, T., Sato, Y., Fujii, A., & Kaneko, S. (2007). Different serum concentrations of steady‐state valproic acid in two sustained‐release formulations. Psychiatry and clinical neurosciences, 61(3), 308-312. https://doi.org/10.1111/J.1440-1819.2007.01656.X

[46] Yang, K., Wan, S., Chen, B., Gao, W., Chen, J., Liu, M., ... & Wu, H. (2016). Dual pH and temperature responsive hydrogels based on β-cyclodextrin derivatives for atorvastatin delivery. Carbohydrate polymers, 136, 300-306. https://doi.org/10.1016/j.carbpol.2015.08.096